Friction driven micromotors with both clockwise and counterclockwise rotations

Bernard Legrand, Lionel Buchaillot, Dominique Collard

Friction driven micromotors with both CW and CCW rotations

Bernard Legrand, Lionel Buchaillot, Dominique Collard

Institut d'Electronique, de Microélectronique et de Nanotechnologie (IEMN – CNRS UMR 8520)
Département ISEN, groupe Microsystèmes Silicium
Cité Scientifique, Avenue H. Poincaré
F-59652 VILLENEUVE D'ASCQ

Résumé :

Cet article présente la réalisation et le fonctionnement d'un micro-moteur angulaire entraîné par friction dont le diamètre du rotor est de 125 µm. La technologie de fabrication est issue des microtechnologies sur silicium avec l'utilisation de silicium polycristallin comme matériau structurel. Les coupleurs mécaniques du moteur sont mis en vibration par des actionneurs électrostatiques à peignes interdigités. Le contrôle du sens de rotation du moteur est obtenu en variant l'amplitude et la fréquence d'excitation des actionneurs, ce qui influe sur la nature de l'interaction entre les coupleurs et le rotor : pure friction dans un cas, ou alors friction et phénomènes d'adhésion. Les applications potentielles de ce type de micro-moteurs tireront partie du couple disponible à basse vitesse permettant de motoriser d'autres micro-mécanismes.

Abstract :

This submission presents friction driven angular micro-motors that demonstrate both clockwise (CW) and counter clockwise (CCW) rotations with a single set of mechanical converters. Fabrication technology is based on surface micromachining of polycrystalline silicon layers in thin films. Rotor diameter is 125 µm and converter vibration is obtained by the use of combdrive actuators. Rotation direction depends on the operating conditions (driving amplitude and frequency of the actuators) that lead to either pure friction or to friction and stiction between the converters and the rotor. Potential applications for driving micro-mechanisms will benefit from a high available torque at low speeds.

Keywords :

MEMS ; Micromotor ; Friction ; Stiction.

1 Introduction

At the micrometric scale, electrostatic driven angular motors have been realized using MEMS technology. However the poor start-up characteristics limit the possibility to transfer energy to other micro-mechanisms [1,2]. On the contrary, vibromotors produce high torque at low speeds, which is a key feature for applications. They convert the vibratory motion of a converter into a continuous linear and angular motion of a rotor by friction contact. Such motors have already been realized down to the millimeter range using piezoelectric stimulated vibratory converters [3]. The same operation principle can be applied to micro-motors with stimulation induced by combdrive actuators. An impact mass is driven either at [4] or out of [5] the resonance frequency to transfer energy through the converter to the rotor. In this submission, we present micro-vibromotors [6] that offer CW and CCW rotations with a single set of mechanical converters. Rotation direction control is obtained by taking advantage of stiction effects between the converters and the rotor that occur at low vibration frequency.

2 Fabrication process and design

2.1 Fabrication process

The fabrication process shown on Figure 1 is based on surface micromachining of two structural layers of polycrystalline silicon (polysilicon). Six mask levels are used for the realization. Starting from a (100) silicon wafer, a 350 nm thermal oxidation is performed, followed by the deposition of a 150 nm thick low stress silicon nitride (Si_xN_y) layer and a 250 nm doped polysilicon layer (P0) (Fig. 1a). This layer is used for the electrical contacts and electrodes that are defined by standard optical lithography on a 1.6 µm thick spin coated resist layer (Shipley S1818). Resulting patterns are transferred to the polysilicon layer P0 by Reactive Ion Etching (RIE) using a $SF_6/CF_4/O_2$ based plasma. The resulting polysilicon electrodes are buried by a 500 nm thick low stress silicon nitride (Si_xN_y) layer and by a 2 µm Low Temperature silicon Oxide (LTO) sacrificial layer. This oxide layer is then patterned by two step optical lithography and RIE etching using a CF_4/CHF_3 gas mixture in order to define bushings and contact holes in the oxide layer (Fig. 1b).

A 2 µm thick diffusion doped polysilicon layer (P1) is subsequently deposited on the wafer. This first structural layer is patterned after optical lithography using chlorine/helium based RIE to obtain vertical sidewalls with no mask underetching, which is a required feature for the combdrive actuators realization (Fig. 1c). A second 2 µm LTO sacrificial layer followed by a second 2 µm polysilicon structural layer (P2) are then deposited and processed in the same way as described just before (Fig. 1d). Stress relaxation in the structural materials is obtained by thermal annealing at 1100 °C during 60 min..

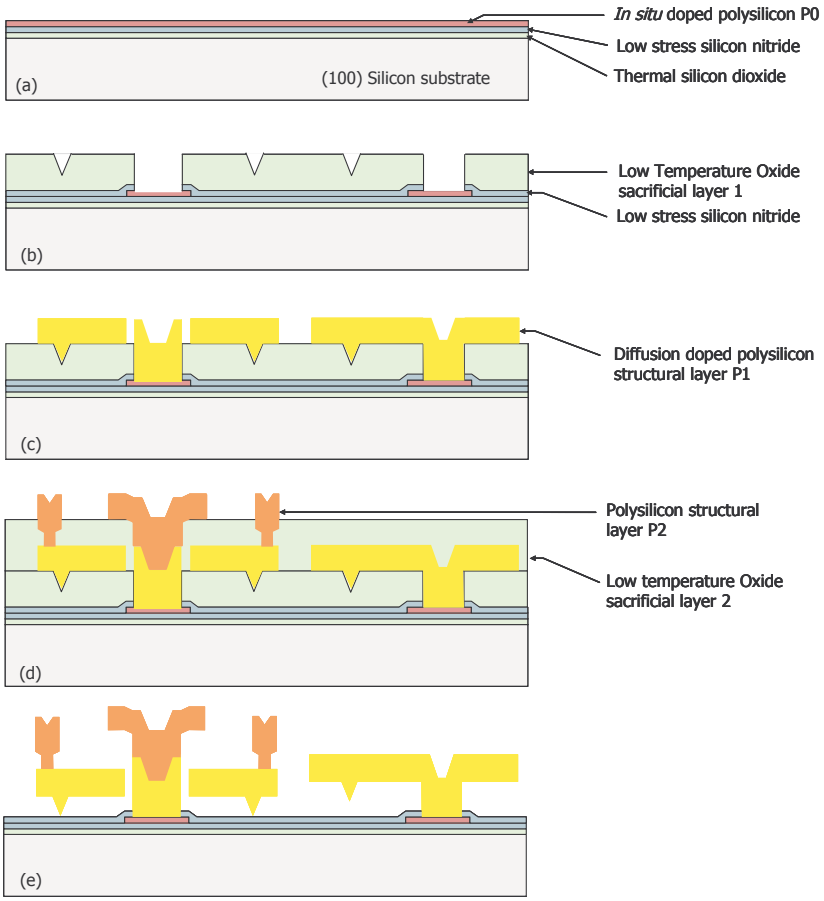

FIG. 1 – Schematic view of the fabrication process based on surface micromachining of two structural levels of polycrystalline silicon.

Structures are released by etching the LTO sacrificial layers in a 49 % HF solution during 20 min., followed by a 20 min. rinsing in de-ionized water and a 20 min. rinsing in isopropylic alcohol (Fig. 1e). Finally, a supercritical CO_2 machine is used to dry the wafer and prevent the released structures from sticking onto the surface.

2.2 Micro-motor design

Figure 2 presents an overview (a) and some details (b, c, d) of a micro-vibromotor. The 125 µm diameter rotor has a 4 µm rim thickness, a shaft diameter of 25 µm and a hub clearance of either 2 or 4 µm. Three dimples provide contact with the ground plane to limit friction. Many converter shapes have been designed and clearance between the converter and the rotor is 2.5 µm. Two combdrive actuators are used for each motor. They are designed to give a 5 µN force for a 40 V voltage supply, which corresponds to a theoretical static torque applied on the rotor of 440 10^{-6} µNm.

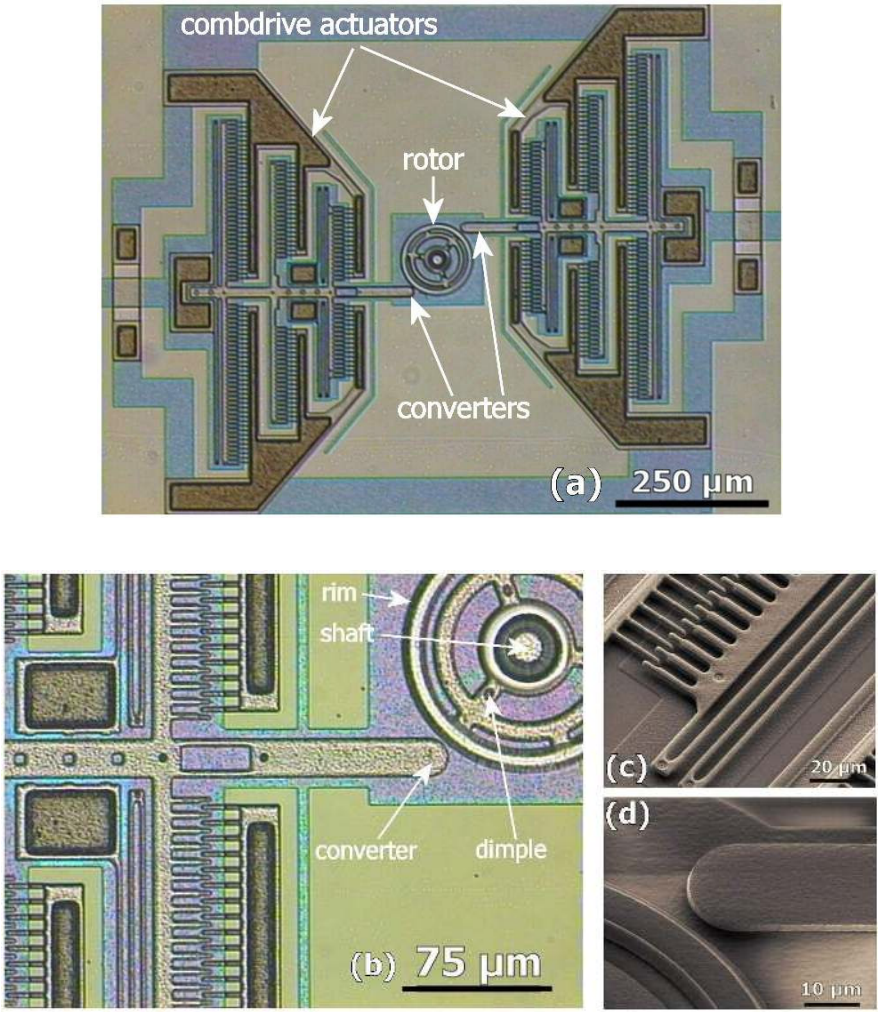

FIG. 2 – (a) Optical microscope image of a micro-motor with its two combdrive actuators. (b) Close view of the rotor and the converter. (c) SEM image of the combdrive actuators and suspension beams. (d) SEM close view of the gap between the rim and the converter.

Suspension beams of the combdrive actuators have been designed using Finite Element Method (FEM) simulations so as to obtain both longitudinal and transversal deflections, which is required for efficient rotor friction driving. Figure 3 (a,b) shows simulation results obtained using ANSYS software. The beam square section is 2 x 2 µm². Selected structure offers longitudinal and transversal stiffness at the converter location of 0.63 Nm^{-1} and 7.25 Nm^{-1} respectively. Figure 3c shows the static deformed shape of the

suspension structure for a large displacement of an actuator which is consistent with the previous FEM simulations.

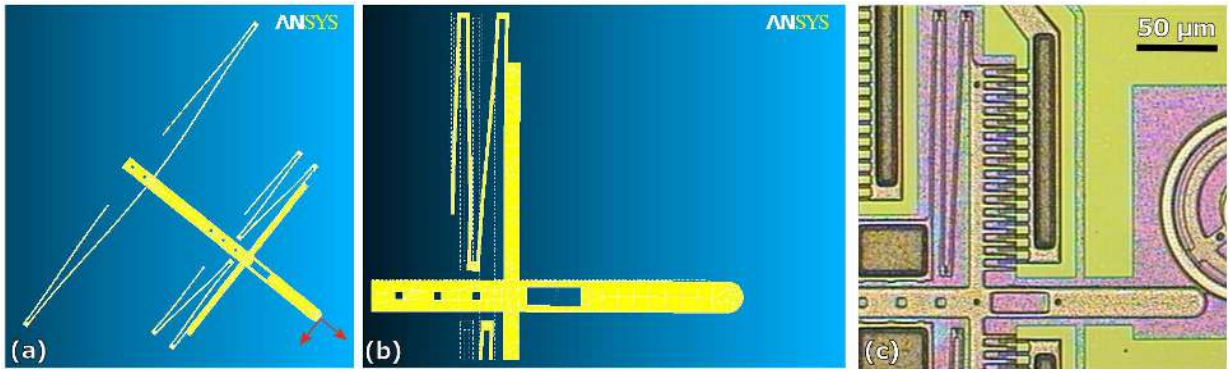

FIG. 3 – (a) ANSYS FEM static simulation of the displacement of the combdrive actuator suspension structure. Red arrows represent the combination of the applied forces. (b) Close view of the resulting deformation of the suspension beams. (c) Optical microscope image of an actuator with a large static force applied to the rotor through the round shaped converter. Note the deformation of the suspension beams.

Electrical excitation is supplied to the combdrive actuators through the electrical interconnects of the polysilicon layer P0. Electrostatic shields are drawn on the P0 layer below the mobile parts and put at the same electrical potential to avoid any pull-in effects between the combdrive actuators and the substrate. Excitation can be supplied either synchronously or not to each of the two combdrive actuators of the micro-motor.

3 Experimental characterizations

3.1 Experimental set-up

Tests are carried out using manual probe heads on a Suss-Microtec PM5 probe station at atmospheric pressure and room temperature with 40 % relative humidity. A standard waveform generator followed by a high voltage amplifier is used to deliver the driving signal to the micro-motors. Peak to peak amplitude of the supplied signal can thus reach +/- 200 V on the 0-1 MHz frequency range.

3.2 Results

First, the combdrive actuators have been characterized. Measured resonance frequency f_0 of the actuators is around 8 kHz, which is consistent with FEM simulations. Displacement versus voltage static characterizations of the actuators are in good agreement with the calculations of the produced electrostatic forces and of the longitudinal stiffness of the suspension beams (see above part 2). For the following experiments, the actuators are driven at frequencies lower than f_0.

Figure 4 shows CCW rotation of a motor fitted with triangle shaped converters under 1 kHz sinusoidal excitation and 20 V peak amplitude. Linear speed of the rim is 300 $\mu m.s^{-1}$, which corresponds to a displacement of 150 nm per converter cycle. In this case, the rotor is driven by both impact and friction phenomena between the converters and the rotor.

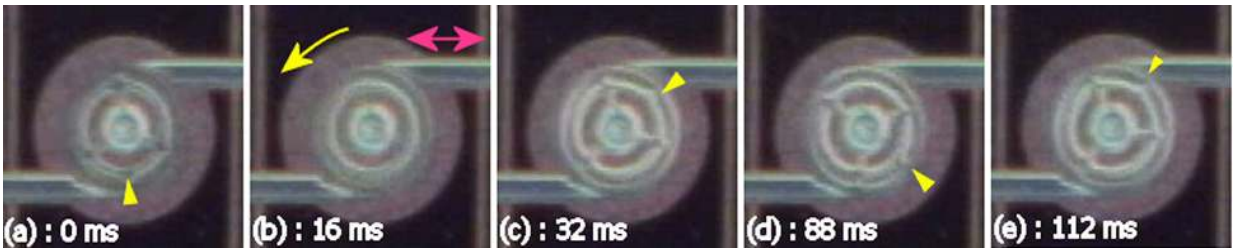

FIG. 4 – Snapshots of a video sequence showing the counter clockwise rotation of the motor due to friction effects at 1 kHz driving excitation. Yellow triangles highlight a mark on the rotor.

Figure 5 shows the same motor under 15 Hz excitation and 30 V amplitude. During the approach of the converters (fig. 5b), friction leads to CCW rotation and transversal flexion of the converters. When the converters are withdrawn a larger CW rotation occurs (fig. 5c) due to adhesion forces between the rotor and the converters. These forces are estimated to be 2 μN. Each converter cycle produces a net rim linear displacement of 4.5 μm.

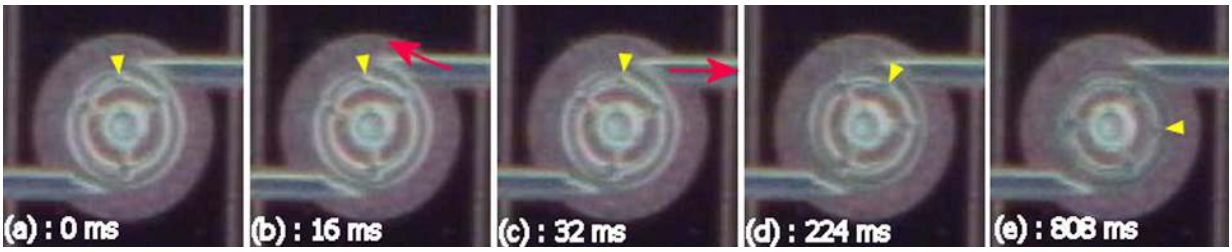

FIG. 5 – Snapshots of a video sequence showing the clockwise rotation of the motor due to stiction effects at 15 Hz driving excitation. Yellow triangles highlight a mark on the rotor.

Figure 6 gives a schematic representation versus time of the micro-motor operation for direct and reverse rotations. Note that the mechanical excitation frequency (Fig. 6b) is twice the electrical driving frequency (Fig. 6a) due to the fact that electrostatic forces depend on the square value of the applied voltage. The fact that adhesion forces leading to CW rotation act only at low frequency (Fig. 6f) can be explained by rotor inertial characteristics : actuator acceleration at high frequency (Fig. 6e) excitation is high enough to prevent the converters from remaining stuck to the rim. Consequently, CCW rotations have only been observed at 15 Hz excitation due to adhesion forces between the converters and the rim.

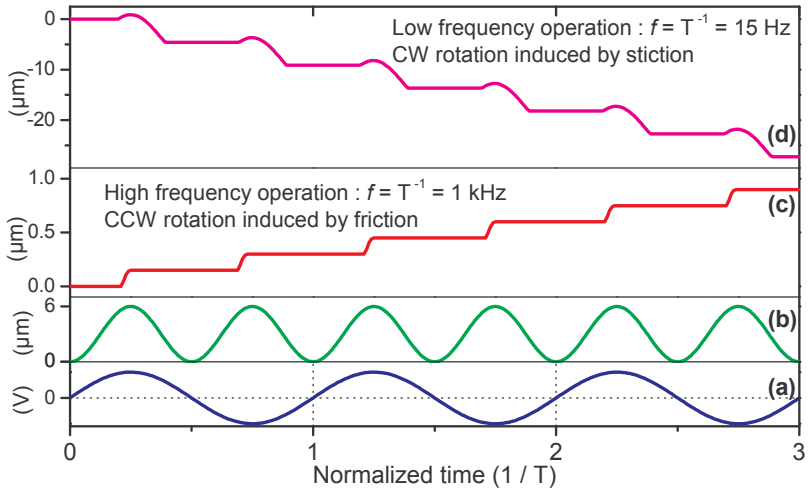

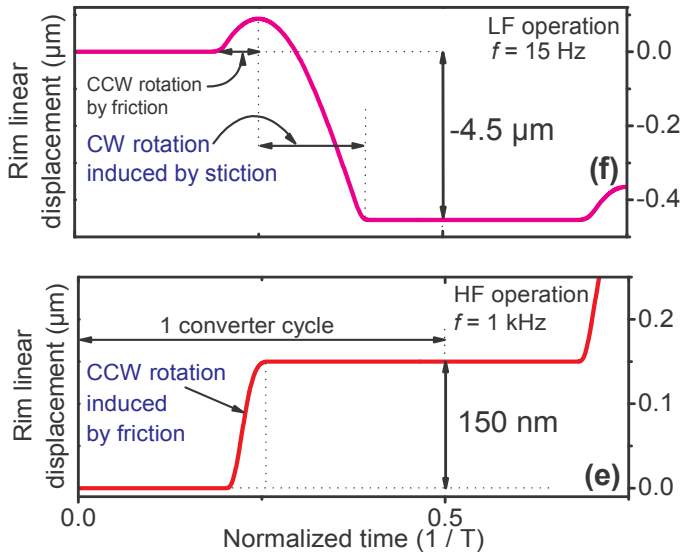

FIG. 6 – Schematic representation versus time of : (a) Micro-motor excitation voltage waveform ; (b) Combdrive actuator theoretical free displacement ; (c) Rim displacement for a high frequency excitation ; (d) Rim displacement for a low frequency excitation.
(e) : Detail of schematic operation of CCW rotation induced by friction effects ; (f) Detail of schematic operation of CW rotation induced by combination of friction and stiction effects.

4 Conclusion

We have demonstrated the fabrication and the characterization of micro-vibromotors that present both CCW and CW rotations with a single set of mechanical converters. CW rotations are obtained at low driving frequency by taking advantage of stiction between the converters and the rotor. Potential applications for micro-mechanisms will benefit from the high available torque.

References

[1] Y.C. Tai and R.S. Muller, *Sensors and Actuators*, A21-23, 1990, 180-183

[2] K.J. Gabriel, F. Behi, and R. Mahadevan, *Sensors and Actuators*, A21-23, 1990, 184-188

[3] M. Fleisher, D. Stein, and H. Meixner, *IEEE Trans. Ultrason., Ferroelec., Frequency Contr.*, 36, 1989, 607-613

[4] M.J. Daneman, N.C. Tien, O. Solgaard, A.P. Pisano, K.Y. Lau, R.S. Muller, *JMEMS*, 5, 3, 1996, 159-165

[5] A.P. Lee, A.P. Pisano, *JMEMS*, 2, 1992, 70-76

[6] L. Buchaillot, French Patent n° 00 06677, 05/25/2000